Optics and Laser Technology 100 (2018) 157–164

Contents lists available at ScienceDirect

Optics and Laser Technology

journal homepage: www.elsevier.com/locate/optlastec

Full length article

Numerical simulation of spatter formation during fiber laser welding of 5083 aluminum alloy at full penetration condition

Dongsheng Wu *, Xueming Hua, Lijin Huang, Jiang Zhao

Shanghai Key Laboratory of Material Laser Processing and Modification (Shanghai Jiaotong University), Shanghai 200240, PR China
Collaborative Innovation Center for Advanced Ship and Deep-Sea Exploration, Shanghai 200240, PR China

ARTICLE INFO

Article history:
Received 26 February 2017
Received in revised form 30 August 2017
Accepted 10 October 2017

Keywords:
Laser welding
Keyhole
Spatter
CFD

ABSTRACT

The droplet escape condition in laser welding is established in this paper. A three-dimensional numerical model is developed to study the weld pool convection and spatter formation at full penetration during the fiber laser welding of 5083 aluminum alloy. It is found that when laser power is 9 kW, the bottom of the keyhole is dynamically opened and closed. When the bottom of the keyhole is closed, the molten metal at the bottom of the back keyhole wall flows upwards along the fusion line. When the bottom of the keyhole is opened, few spatters can be seen around the keyhole at the top surface, two flow patterns exists in the rear part of the keyhole: a portion of molten metal flows upwards along the fusion line, other portion of molten metal flows to the bottom of the keyhole, which promote the spatter formation at the bottom of the keyhole rear wall.

1. Introduction

When a high intensity laser beam impinges on the base metal, the surface temperature of material quickly increases, which can cause the melting and evaporation of the material. Under the influence of recoil pressure caused by evaporation, the molten metal is extruded, a deep keyhole is formed [1]. The spatter is generated when the momentum of a local volume of molten metal is high enough to overcome the surface tension force. The formation of spatter can also lead to other defects, such as underfilling and undercutting [2].

Fabbro investigated the effect of the interaction between molten pool and vapor that generated at the front keyhole wall in Nd-YAG laser welding, and found that the drag force caused by vapor could accelerate the molten metal around the keyhole, the spatter generation could be suppressed by using adequate side gas jet nozzle [3]. Kawahito proposed that the strong shear force of laser induced plume rather than recoil pressure of metallic vapor was responsible for the formation of spatter, the spatter could be reduced by controlling the direction of laser induced plume [4]. Weberpals used high speed video camera to observe the spatter formation, and founded that the maximum ejection angle of droplets emitted from the rear part of the keyhole rim had linear relationship with keyhole front wall inclination [5]. Kaplan developed a systematic description of various types of spatter phenomenon in laser welding, and proposed a categorization system to facilitate the comparison and combination of research findings on spatter [6]. Zhang used a modified "sandwish" specimen to observe the geometry of the keyhole wall, he proposed that the recoil momentum associated with the energized vapor plume jet were responsible for the formation of high speed micro-spatter [7]. Li used the high speed video cameras to observe the weld pool of glass and steel behind the keyhole, he proposed that the breaking of vapor generated wave was the key to explain the generation mechanism of swelling, and spatter in high power deep penetration laser welding [8]. He also used a X-ray transmission imaging system to investigate the weld pool convection in the laser welding, and found that the behavior of the weld pool was the key factor to determine the spatter formation [9].

Due to its excellent resistance to corrosion, weldability and formability, 5083 aluminum alloy is widely used in modern high speed train, liquefied natural gas (LNG) carrier and shipbuilding manufacturing industry. It is inevitable to join 5083 aluminum alloy by various welding methods, such as laser welding. However spatter may be generated during the laser welding process, which can deteriorate the weld quality. It has certain significance to study the formation mechanism of spatter in laser welding of 5083 aluminum alloy, and adopt reasonable measures to reduce it. Due to the lower viscosity and low surface tension, the spatter behavior in laser welding of aluminum alloy is very different from that in

* Corresponding author at: Shanghai Key Laboratory of Material Laser Processing and Modification (Shanghai Jiaotong University), Shanghai 200240, PR China.
E-mail address: 767057108@qq.com (D. Wu).

https://doi.org/10.1016/j.optlastec.2017.10.010
0030-3992/

laser welding of steel [10]. However, the studies on investigating the spatter formation in laser welding of aluminum alloy are very limited [11]. Besides, very few investigations are carried out to study the weld pool convection and spatter formation at full penetration during laser welding of aluminum alloy.

In this article, the droplet escape condition is built, a high speed video camera is used to observe the spatter formation, a three-dimensional numerical model is established to investigate the fluid flow features within the weld pool, and spatter formation at full penetration during the fiber laser welding of 5083 aluminum alloy.

2. Experimental procedure

The experimental set-up used for the experiments is shown in Fig. 1. The experiments are performed using a fiber laser welding machine (IPG 1000), whose maximum output power is 10 kW, output wavelength is 1070 ± 10 nm, the focal radius of laser beam is 0.36 mm. The material used is 5083 aluminum alloy plate with length 120 mm, width 40 mm, thickness 10 mm, the thermo-physical material properties of the base metal is shown in Table 1. Before welding, the plates are scratch brushed, and then cleaned by acetone. During the welding, the laser power is 9 kW, the defocused distance is 0 mm, the welding speed is 2 m/min, pure argon gas is used as shielding gas with a flow rate of 20 L/min, the nozzle is placed at the trailing position with a typical inclination of 45°.

During the welding, a high speed video camera is used to observe the weld pool behavior and spatter formation, a band pass filter with a transmission band of 808 nm is positioned in front of the camera lens to filter out unwanted arc light, the frequency is 5000 frame/s. In order to observe the weld pool, a diode laser (λ = 806 ± 10 nm) with a maximum power of 300 W is used to illuminate the welding zone.

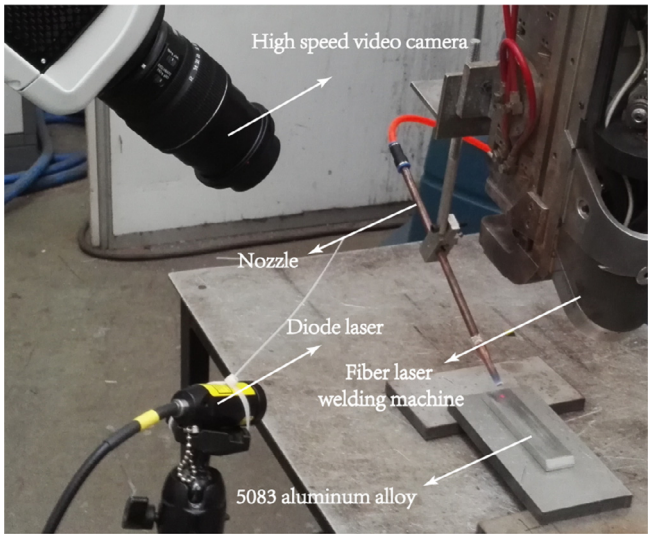

Fig. 1. Diagram of the experimental platform.

The weld seam appearances are shown in Fig. 2. It can be seen that the weld seam is fully penetrated when the laser power is 9 kW, the number and size of the spatters in bottom surface is larger than that in top surface.

3. The droplet escape condition

3.1. Young-Laplace equation

The surface tension pressure of a curved surface can be obtained from the Young-Laplace equation. As shown in Fig. 3, AB is a raised liquid surface, the radius is r, the perimeter of AB bottom surface is $2\pi r$, the area of AB bottom surface is πr^2, the radius of the sphere is R. The liquid surface tension is γ, the component in horizontal direction is $\gamma\sin\alpha$, the component in vertical direction is $\gamma\cos\alpha$, the sum of liquid surface tension in vertical direction is $\gamma\cos\alpha \cdot 2\pi r$. So the surface tension pressure of the raised liquid surface is $\Delta p = \gamma\cos\alpha \cdot 2\pi r/\pi r^2$. For $\cos\alpha = r/R$, so we can get:

$$\Delta p = 2\gamma/R$$

The radius R needs to be considered in both dimensions at the surface location. If both radii are equal, this factor two appears. Otherwise it would be $(\gamma/R_1 + \gamma/R_2)$ for two different radii.

3.2. The droplet escape condition

The droplet escape condition is obtained by comparing the stagnation pressure of the melt with the surface tension pressure of a curved surface. The magnitude of stagnation pressure can be derived from a simplified form of Bernoulli equation. For incompressible flow, $P_{stagnation} = \rho v^2/2$.

Where ρ is fluid density, v is the vertical component of the velocity, normal to the surface at a certain location.

When the stagnation pressure of the melt is larger than the surface tension pressure, the droplets are generated. That is $\rho v^2/2 \geq 2/R$.

4. Mathematical model and numerical simulation

Some assumptions have been made to simplify the mathematic model: (1) The flow is laminar, the liquid metal is considered to be a Newtonian and incompressible fluid. (2) The vapor flow inside the keyhole is ignored. (3) The effect of shielding gas on welding process is omitted. (4) The heat source of laser beam is modeled as Gaussian density distribution.

4.1. Governing equations

The weld pool simulation of laser welding is based on the numerical simulation of mass, momentum, and energy equations.

Table 1
Thermo-physical material properties of 5083 aluminum alloy.

Nomenclature	Value	Nomenclature	Value
Density (l)	2380 (kg/m^3)	Thermal conductivity (s)	235 (W/m·K)
Density (s)	2660 (kg/m^3)	Liquidus temperature	933 (K)
Viscosity	4.2×10^{-3} (kg/m·s)	Solidus temperature	847 (K)
Specific heat (l)	1197.21 (J/kg·K)	Heat transfer coefficient	20 (W/m^2·K)
Specific heat (s)	1050 (J/kg·K)	Coefficient of thermal expansion	1.5×10^{-4} (K^{-1})
Latent heat of fusion	3.87×10^5 (J/kg)	Surface tension	0.871 (N/m)
Thermal conductivity (l)	90 (W/m·K)	Surface tension gradient	−0.000155 (N/m·K)